4th International Conference on Experiments/Process/System Modeling/Simulation/Optimization
4th IC-EpsMs0
Athens, 6-9 July, 2011

NUMERICAL SIMULATION IN VERTICAL WIND AXIS TURBINE WITH PITCH CONTROLLED BLADES

Bayeul-Lainé Annie-Claude[1], Dockter Aurore[2], Bois Gérard[3], Simonet Sophie[4]

[1] LML, UMR CNRS 8107, Arts et Metiers PARISTECH
8, Boulevard Louis XIV 59000 Lille, France
e-mail : annie-claude.bayeul-laine@ensam.eu

[2] e-mail : aurore.dockter-9@etudiants.ensam.eu

[3] e-mail : gerard.bois@ensam.eu

[4] e-mail : sophie.simonet@ensam.eu

Keywords: numerical simulation, performance coefficient, unsteady simulation, VAWT, vertical axis, wind energy, pitch controlled blades

Abstract: Wind energy is more and more used as a renewable energy source character. The present wind turbine is a small one which allows to be used on roofs or in gardens to light small areas like publicity boards, parking, roads or for water pumping, heating... The present turbine has a vertical axis. Each turbine blade combines a rotating movement around its own axis and around the main rotor axis. Due to this combination of movements, flow around this turbine is highly unsteady and needs to be modeled by unsteady calculation. One of the main problems of such geometry is to simulate the two combined movements. The present work is an extended study of one's made in 2009. In the previous study, some results like contours of pressure and velocity fields were presented for elliptic blades for one specific constant rotational speed and benefits of combined rotating blades was shown. The present paper points up the influence of two different blades geometries for different rotational speeds, different blade stagger angles and different Reynolds numbers related to a wider range of wind speeds.

1 INTRODUCTION

All wind turbines can be classified in two great families (refs. [8,9…]): horizontal-axis wind turbine (HAWTs) and vertical-axis wind turbine (VAWTs)The present study concerns a small VAWT technology in which each blade combines a rotating movement around its own axis and a rotating movement around turbine's axis. A lot of works was published on VAWTs like Savonius or Darrieus rotors ([7, 8,10…]) but few works were published on VAWTs with rotating blades ([2, 3, 4, 5, 6]). Some inventors discovered this kind of turbine in the same time on different places ([4, 5, 6] for example). This paper concerns an industrial one used to light publicity panel: in 2008, F. Penet, P. de Bodinat and J. Valette gained an innovation price for an idea in which this kind of turbine is used to make a publicity panel lighted by wind energy. They created the society Windisplay to design, create and send such a product.

The common non dimensional coefficients used for all wind turbines are:

- Efficiency of a rotor, named power coefficient C_p

$$C_p = \frac{P_{eff}}{\frac{\rho S V_0^3}{2}} \tag{1}$$

In which P_{eff} is the power captured by the turbine and $\frac{\rho S V_0^3}{2}$ is the total kinetic energy passing through the swept area (Figure 3).

- Speed ratio

$$\lambda = \frac{\omega R_t}{V_0} \tag{2}$$

Where ω the angular velocity of the turbine is, R_t is generally the radius blade tip and the radius of center of blade in case of this paper and V_0 the wind velocity.

- Reynolds number ([1, 12] based on blade's length

$$R_e = \frac{V_0 \, L}{\nu} \tag{3}$$

Some results were presented last year with elliptic blades. To resume these last studies, the benefit of rotating blades was confirmed: the performance of this kind of turbine was very good as expected, better than those of classical VAWTs for blade stagger angle comprised between 0 and 15 degrees. It was shown that each blade behavior has less influence on flow stream around next blade and on power performance. The maximum mean numerical coefficient was about 32%.

The blade sketch needs to have two symmetrical planes because the leading edge becomes the trailing edge when each blade rotates once time around the turbine's axis. In the present study, new simulations were performed with straight blades. Results are compared between elliptic blades and straight blades: local results like contours of pressure, velocity fields, unsteady power coefficient, mean power coefficient.

2 GEOMETRY AND TEST CASES

The sketch of the industrial product is shown in figure 1. Blades have elliptic or straight sketches and relatively height, so a 2D model was chosen. The calculation domain around turbine is large enough to avoid perturbations as showing in Figure 2. Elliptic forms have minor radius of 75 mm and major radius of 525mm. Straight forms have a length of 1050 mm. Distance between turbine axis and blade axis is 620 mm.

Boundary conditions are velocity inlet to simulate a wind velocity in the lower line of the model (7.8e4<Re<5.6e5), symmetry planes for right and left lines of the domain and pressure outlet for the upper line of the domain. The model contains five zones: outside zone of turbine, three blades zones and zone between outside zone and blades zones named turbine zone. Turbine zone has a diameter named D (equal to the sum of R, plus the major radius of blade plus a little gap allowing grid mesh to slide between each zone). Except outside zone, all other zones have relatively movements. Four interfaces between zones were created: an interface zone between outside and turbine zone and an interface between each blade and turbine zone. Details of zones are given in Figure 2.

Figure 1 sketch of the VAWT studied

Previous calculations, realized last year, for an initial blade stagger angle α comprised between -30 and 30 degrees showed that flow is highly unsteady for α equal -30 or 30 degrees. So, new calculations were performed for three initial blade stagger angles of 0, 8 and 15 degrees as it can be seen in figure 3.

Mesh was refined near interfaces. Prism layer thickness was used around blades. The resulting computational grid is an unstructured triangular grid of about 60 000 cells, as shown in Figures 2 and 3.

A time step corresponding to a rotation of 6.28e-3 radians was chosen to avoid to deform more quickly mesh near interfaces and so, to avoid negative cells. So a new mesh was calculated at each time step.

All simulations were realized with Star CCM+ V5.02 code using a k-ε model.

Fields of pressure and velocity, Forces and Torques on each blade have been recorded during six periods for elliptic blades and three periods for straight blades. Previous studies have shown a good periodicity of flow stream and global results for an initial blade stagger angle of 0 and 15 degrees so it has been supposed that three periods are enough for new calculations.

In a first part, results for an initial blade stagger angle of 15 degrees, for a speed ratio of 0.6 and for Re equal to 560 000 are presented. Contours of pressure near turbine zone are compared between the two types of blades.

In a second part, global results like performance coefficients are compared between the two types of blades and for different Reynolds numbers : 77 800, 155 000, 291 000 and 560 000, for different speed ratios : 0.2, 0.4, 0.6 and 0.8 and for different blade stagger angles : -30, 0, 8, 15 and 30 degrees.

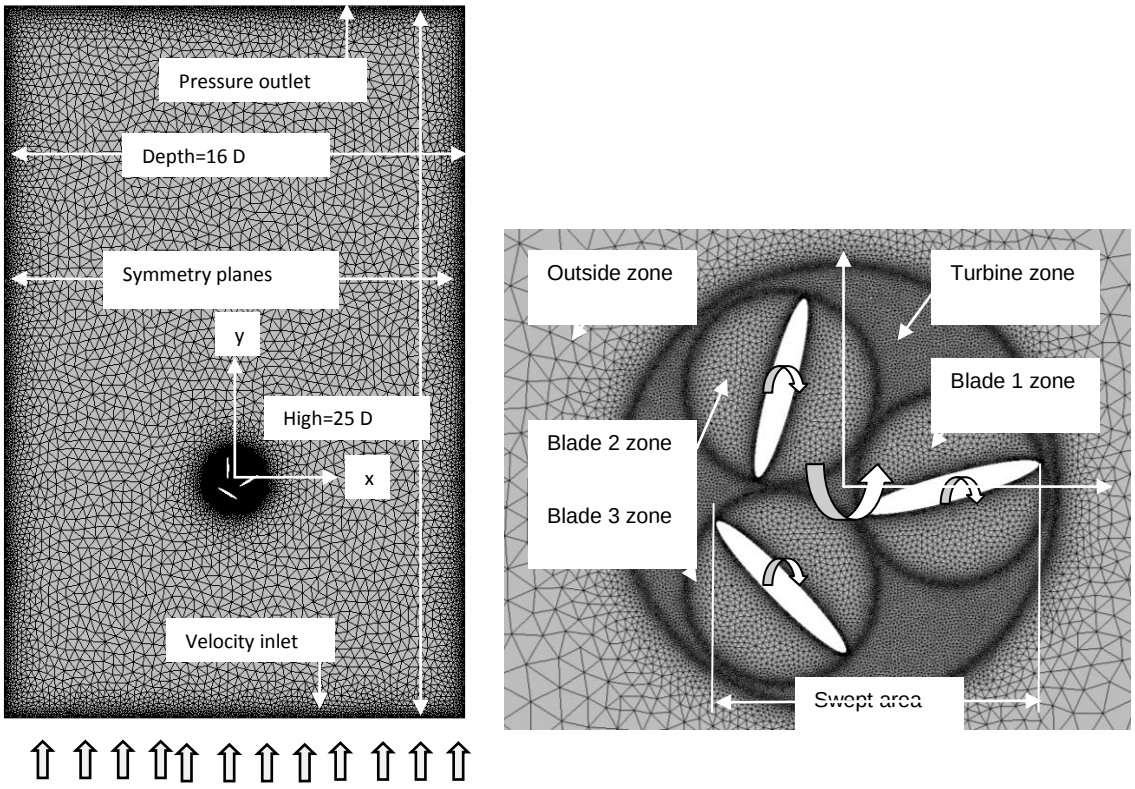

Figure 2 mesh and boundaries' conditions of VAWT with elliptic blades studied

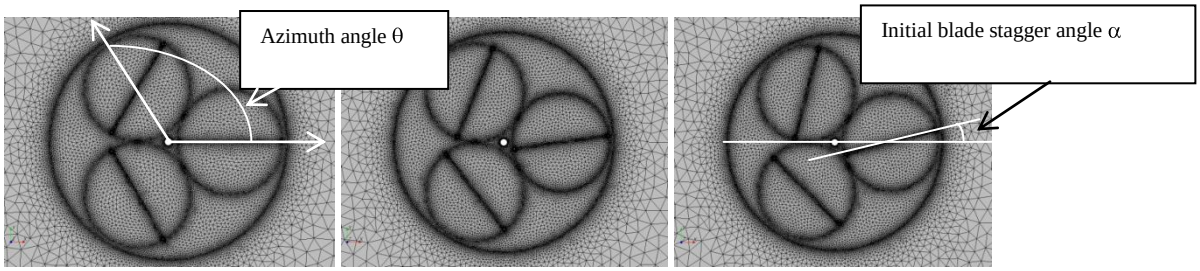

Figure 3 zoom of the mesh of VAWT with straight blades for blade stagger angle of 0, 8 and 15 degrees

3 TORQUES AND POWER COEFFICIENTS

For this kind of turbine each blade needs energy to rotate around its own axe so real power captured by the turbine has to be corrected.

Code gives torque M_t around turbine axis for each blade, pressure forces and viscosity forces. So

$$M_{ti} = \iint_{\text{bladei}} O\vec{G}_i \wedge d\vec{f} + \iint_{\text{bladei}} G_i\vec{M} \wedge d\vec{f} \quad (4)$$

Where O is the turbine center, G_i the axis center of blade i and $\vec{df}$ is elementary force on the blade i due to pressure and viscosity, so

$$M_{ti} = C_{1i} + C_{2i} \quad (5)$$

With

$$C_{1i} = C_1\,\text{blade}i = \iint_{S\,\text{blade}i} O\vec{G}_i \wedge d\vec{f} \tag{6}$$

And

$$C_{2i} = C_2\,\text{blade}i = \iint_{S\,\text{blade}i} G_i\vec{M} \wedge d\vec{f} \tag{7}$$

Real power was given by:

$$P_{eff} = \sum_{i=1,2,3} M_{ti}\,\omega_1 + \sum_{i=1,2,3} C_{2i}\,\omega_2 \tag{8}$$

With ω_1, angular velocity of turbine and ω_2 relative angular velocity of each blade around its own axis
As

$$\omega_2 = {}^{-\omega_1}\!/_{2} \tag{9}$$

$$P_{eff} = \sum_{i=1,2,3} \left(M_{ti} + C_{1i}\right) \frac{\omega_1}{2} \tag{10}$$

And power coefficient by equation (1) in which swept area is those showed in figure 3 for the cases with three rotating blades

4 RESULTS

4.1 Contours of pressure

Figures 4 to 7 give contours of relative pressure for elliptic blades and figures 8 to 11 give same results for straight blades for the maximum Reynolds number corresponding to a wind velocity of 8 m/s, for a speed ratio of 0.6 and for an initial blade stagger angle of 15 degrees. For these values, results are periodic with no highly instabilities. So, only results between 0 to 120 degrees are presented.

In figures 4 to 7, scale between -200 to 100 Pa is used; in figures 8 to 11 scale between -200 to 80 Pa is used. Comparisons between two kinds of profiles show quite same behavior but emphasized in case of straight blades.

For each kind of blades, a swirl arises at the leading edge of the lower blade (figures 4 and 8). This swirl grows when the blade rotates (figures 5, 6, 9 and 10). The swirl breaks off blade for azimuth angle of blade θ equal about -14 degrees and reduces until vanished for θ equal about 90 degrees. In figure 4, two swirls can be observed, the first near the leading edge which has broken off the blade and the second quite above the first which is vanishing.

As it can be observed in the previous studies, blades for azimuth angle between 90 to 250 degrees seem to slide in the flow field avoiding to disturb the flow stream of the wind and avoiding to generate a negative torque as it can be seen in the next part.

4.2 global performances

In this second part, instantaneous results are first presented to show the influence of parameters (blades geometries, initial blade stagger angles, blade speed ratios and Reynolds numbers).

Figure 12 presents evolution of torques with azimuth angle θ of blade 1 for an initial blade stagger angle of 15 degrees and for Reynolds number of 560 000 for the two kinds of blades. Comparison between these results show that straight blades is more influenced by low and high blade tip ratio than elliptic blades: instabilities can be observed in figure 12.2.

Figures 13 give instantaneous power coefficients with azimuth angle of blade 1 for straight blades. Comparison between figures 13.1 and 13.2 shows a very little influence of Reynolds numbers: results are quite similar.

Figures 13.3 and 13.4 confirm that low (λ=0.2) and high (λ=0.8) blade speed ratios lead to very bad performance for straight blades: it can be observed that mean values decrease and that range of change increases, this leads to increase instabilities and to emphasis phenomenon like birth of swirls which disturb flow stream and performances of turbine.

Comparison between figures 13.4 and 14 shows the disadvantage of straight blades for an initial blade stagger angle of 15 degrees: a significant decrease of power coefficient and a significant increase of range of change and of instabilities can be observed between straight and elliptic blades.

The low influence of Reynolds number is confirmed in figure 15 which gives mean power coefficients for different initial blade stagger angles with Reynolds numbers for straight blades. It can be observed a small increase of mean power coefficient with Reynolds number.

Finally figure 15 gives mean power coefficients for all test cases, for elliptic (EB) and straight blades (SB).

This figure summarizes all remarks already made:

- Low influence od Reynolds number (same color curves but with different styles)
- Bad influence of straight blades comparatively to elliptic blades for an initial blade stagger angle of 15 degrees (brown and blue curves can be compared)
- Better influence of straight blades comparatively to elliptic blades for an initial blade stagger angle of 0 degree (red and pink curves can be compared). Maximum mean power coefficient is better for straight blades but it decrease quickly when blade speed ratio decrease or increase from the value 0.4
- Better stability of results for elliptic profile.

Elliptic blades, $\lambda = 0.6$, Re = 5.6^e5	Straight blades, $\lambda = 0.6$, Re = 5.6^e5
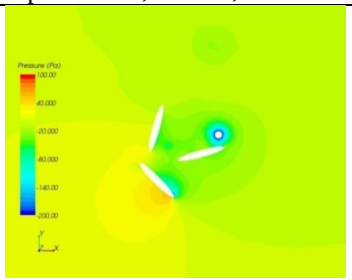	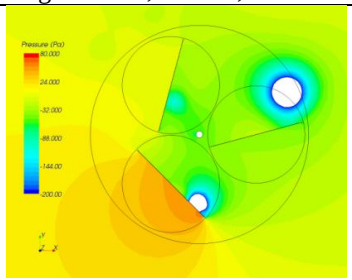
Figure 4 Contours of pressure θ = 0 degree	Figure 8 Contours of pressure θ = 0 degree
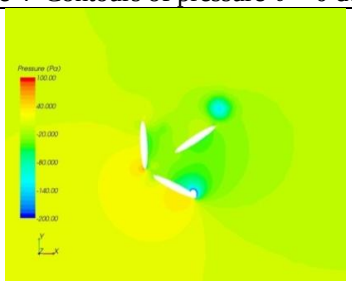	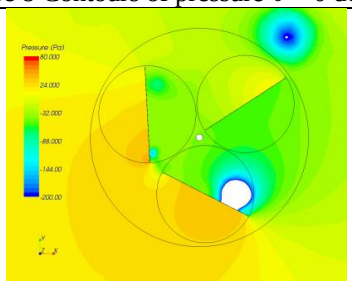
Figure 5 Contours of pressure θ = 36 degrees	Figure 9 Contours of pressure θ = 36 degrees
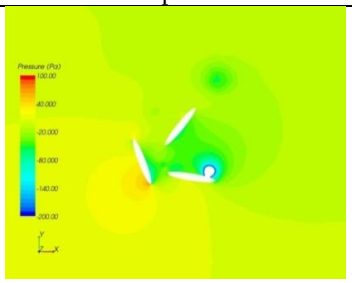	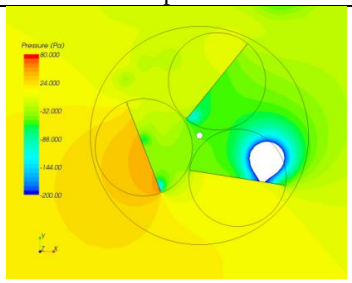
Figure 6 Contours of pressure θ = 72 degrees	Figure 10 Contours of pressure θ = 72 degrees
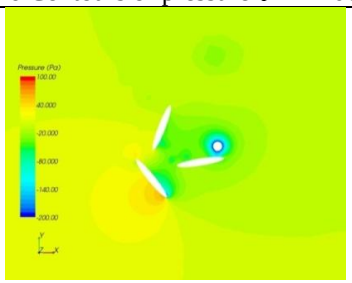	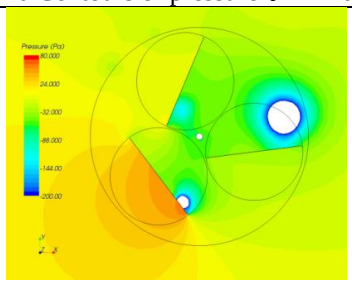
Figure 7 Contours of pressure θ = 108 degrees	Figure 11 Contours of pressure θ = 108 degrees

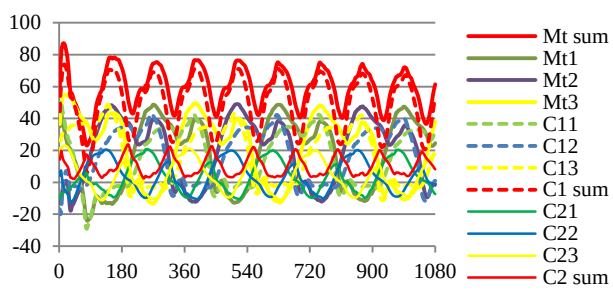

Figure 12.1 Elliptic blades λ=0,2

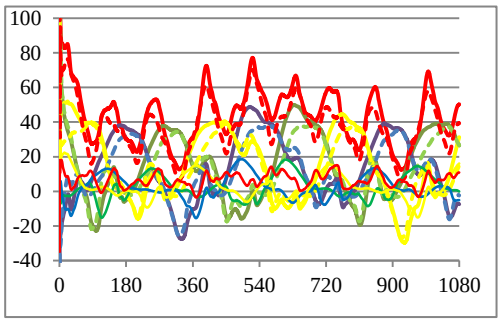

Figure 12.2 straight blades λ=0,2

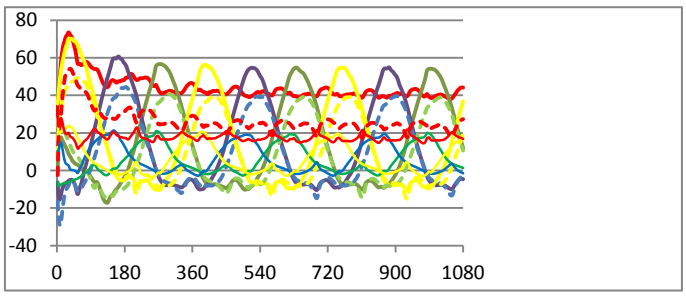

Figure 12.3 Elliptic blades λ=0,4

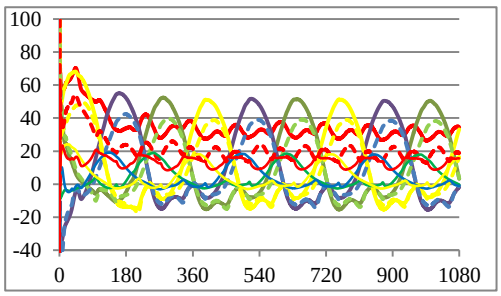

Figure 12.4 Straight blades λ=0,4

Figure 12 Torques (mN/m) for initial blade stagger angle of 15 degrees with azimuth angles of blade 1 Re=5,6e5

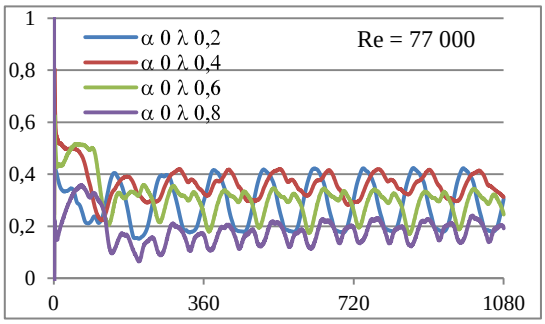

Figure 13-1

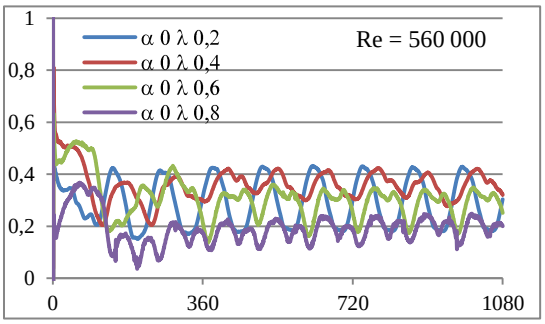

Figure 13-2

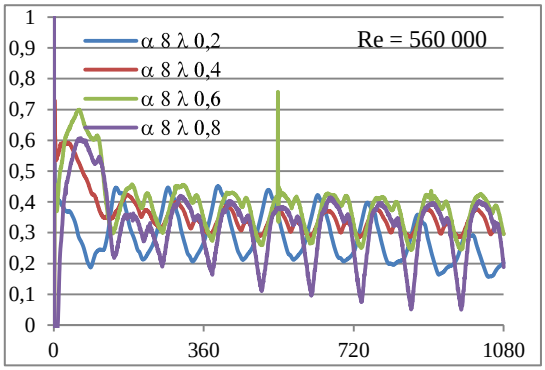

Figure 13-3

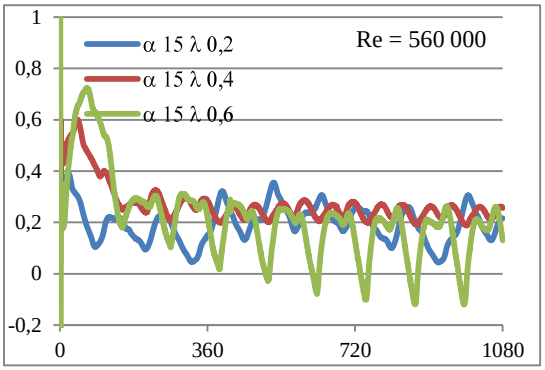

Figure 13-4

Figure 13 instantaneous power coefficients with azimuth angles of blade 1- Straight blades

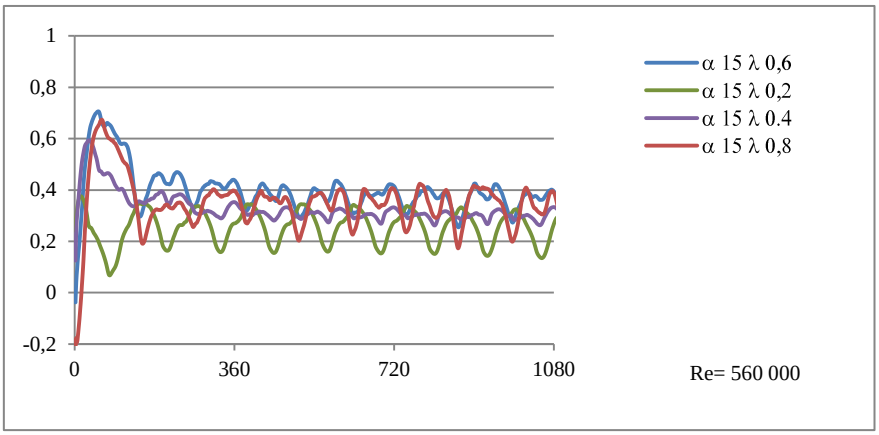

Figure 14 instantaneous performance coefficients with azimuth angle of blade 1- Elliptic blades

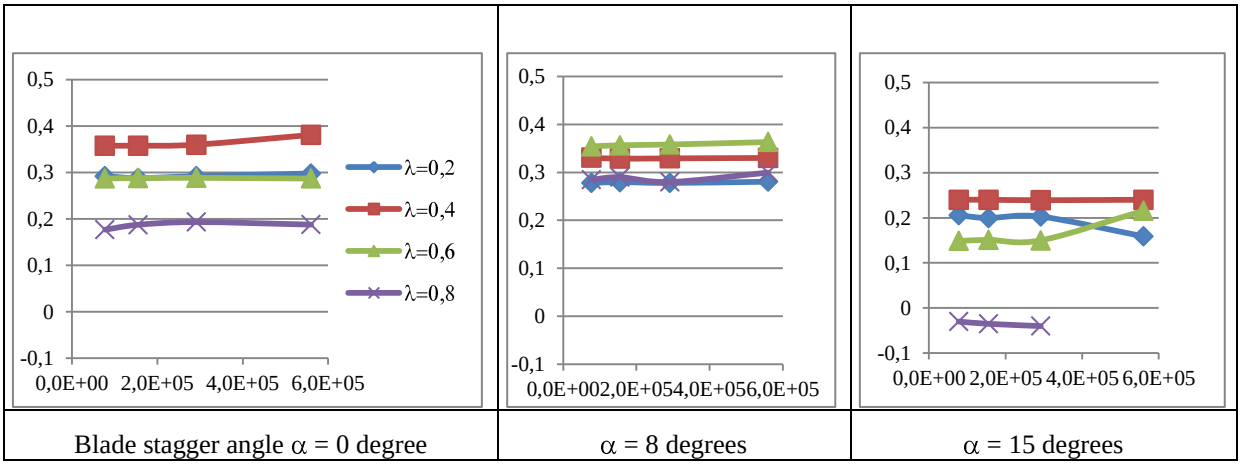

Figure 15 mean power coefficients for different initial blade stagger angles with Reynolds number Straight blades

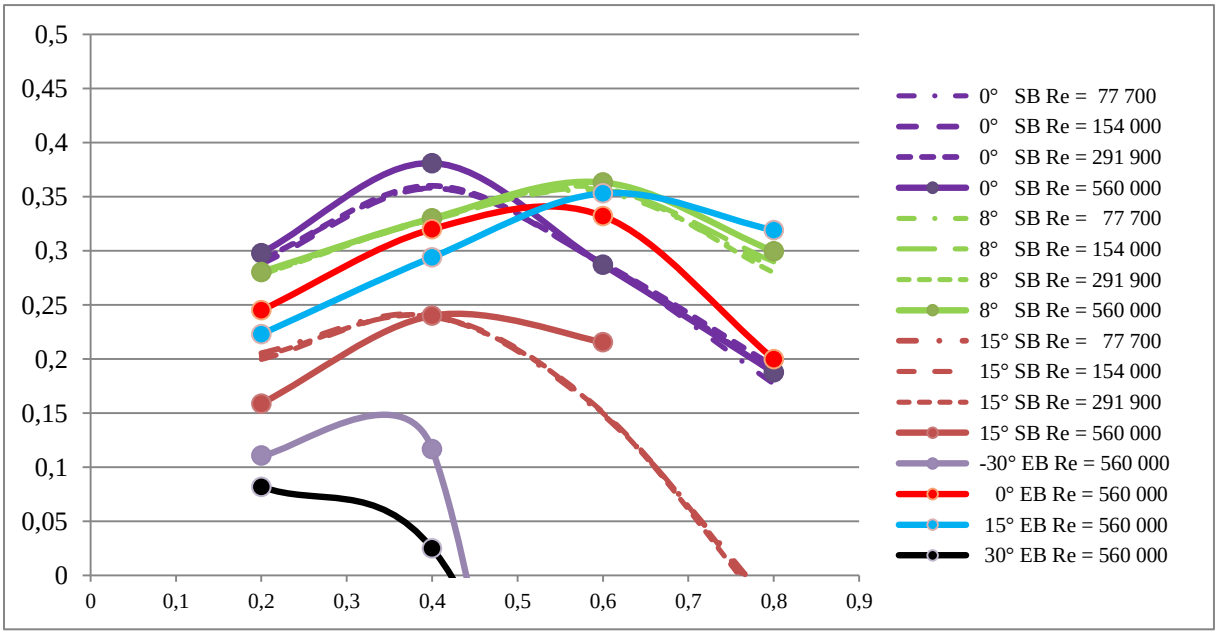

Figure 16 Mean power coefficients for all test cases with blade speed ratios λ

5 CONCLUSION

New numerical experiments were carried out to study the influence of different parameters on the performance of turbines with rotating blades; the following conclusions can be drawn:

- The performance of this kind of turbine is confirmed to be very good and better than those of classical VAWTs for some specific blade stagger.
- The maximum mean numerical coefficient at λ=0.4 was about 38%

A lot of work has still to be done:

- The study of influence of the number of blades to confirm that the relative rotation of blade increase the power performance because each blade doesn't disturb the next blades and to estimate for what number of blades this is right.
- The study of the influence of geometrical parameters like the radius of axis of blades, other kind of design for blade, the choice of this design with the consideration that each side of blade is useful for publicity
- confirm these numerical results by an experimental apparatus in an open-circuit type wind tunnel
- The spectral analysis of unsteady results...

NOMENCLATURE

c_p power coefficient (no units)
C_{eff} real torque (mN)
D diameter of turbine zone (m)
G_i center of rotation of blade i
L length of blade (m)
M_{ti} torque of blade i by turbine axis (mN)
O center of rotation of turbine in 2D model
P_{eff} real power
R radius of axis of blades, (=0.62 m)
R_e Reynolds number based on length of blade
R_t radius of blade tip (m)
S captured swept area (m^2)
V_0 wind velocity, (=8 m/s)
α blade stagger angle (degrees)
λ blade or tip blade speed ratio (no units)
ρ density of air (kg/m^3)
θ azimuth angle of blade 1(degrees)
ω_1 angular velocity of turbine (rad/s)
ω_2 angular velocity of pales (rad/s)

Subscripts

i blade index

REFERENCES

[1] Abbott I. H. , Von Doenhof f A. E. (1949), *Theory of wing sections*, Mc Graw Hill Book, ISBN 486-60586-8
[2] Bayeul-Lainé A. C., Bois G., Simonet S. (2010) , « Etude numérique instationnaire d'une micro-éolienne à axe vertical », 1ère Conférence Fanco syrienne sur les énergies renouvelables, octobre , Damas, Syrie
[3] Bayeul-Lainé A.C., Bois G. (2010), « Unsteady simulation of flow in micro vertical axis wind turbine », *Proceedings of 21st International Symposium on Transport Phenomena, Kaohsiung City Taiwan, 02-05 november*,
[4] Cooper P., Kennedy 0., (2005) "Development and analysis of a novel Vertical Axis Wind Turbine", http://www.datataker.com/public_domain/PD71%20Development%20and%20analysis%20of%20a%20novel%20vertical%20axis%20wind%20turbine.pdf, read in September 2010
[5] Cooper P. (2010), *Wind Power Generation and wind Turbine Design* , WIT Press, chapitre 8, ISBN 978-1-84564-205-1
[6] P.A.M. Dieudonné P.A.M. (2006), « Eolienne à voilure tournante à fort potentiel énergétique », Demande de brevet d'invention FR 2 899 286 A1, brevet INPI 0602890, 03 avril 2006
[7] Hau E. (2000), *Wind turbines*, Springer, Germany
[8] Leconte P., Rapin M., Szechenyi E. (2001), *Eoliennes*, Techniques de l'ingénieur BM 4 640,, pp 1-24
[9] Martin J. (1987), *Energies éoliennes*, Techniques de l'ingénieur B 8 585, pp 1-21
[10] Paraschivoiu I. (2002), « Wind Turbine Design with Emphasis on Darrieus Concept », *Polytechnic International Press*, 2002
[11] Pawsey N.C.K. (2002), "Development and evaluation of passive variable-pitch vertical axis wind turbines, PhD Thesis, Univ. New South Wales, Australia
[12] Marchaj C. A. (2000), *The Aero-Hydrodynamics of Sailing*, International Marine Publishing Company, ISBN 0229986528